Journal of Peptide Science
J. Pept. Sci. 2007; **13**: 504–512
Published online 6 July 2007 in Wiley InterScience (www.interscience.wiley.com). DOI: 10.1002/psc.872

JOURNAL OF PEPTIDE SCIENCE

Structure–function relationship studies of PTH(1–11) analogues containing sterically hindered dipeptide mimetics

NEREO FIORI,[a] ANDREA CAPORALE,[a] ELISABETTA SCHIEVANO,[a] STEFANO MAMMI,[a] ARMIN GEYER,[b] PETER TREMMEL,[b] ANGELA WITTELSBERGER,[c] IWONA WOZNICA,[c] MICHAEL CHOREV[d] and EVARISTO PEGGION[a]*

[a] University of Padova, Department of Chemical Sciences, Institute of Biomolecular Chemistry, CNR, Italy
[b] Philipps Universität, Marburg Fachbereich Chemie, Germany
[c] Tufts University School of Medicine, Department of Physiology, USA
[d] Harvard Medical School, Laboratory for Translational Research, USA

Received 2 March 2007; *Revised 29 March 2007*; *Accepted 10 April 2007*

Abstract: The *N*-terminal 1–34 fragment of parathyroid hormone (PTH) is fully active *in vitro* and *in vivo* and reproduces all biological responses characteristic of the native intact PTH. In order to develop safer and non-parenteral PTH-like bone anabolic agents, we have studied the effect of introducing conformationally constrained dipeptide mimetics into the *N*-terminal portion of PTH in an effort to generate miniaturized PTH-mimetics. To this end, we have synthesized and conformationally and biologically characterized PTH(1–11) analogues containing 3*R*-carboxy-6*S*-amino-7,5-bicyclic thiazolidinlactam (7,5-bTL), a rigidified dipeptide mimetic unit. The wild type sequence of PTH(1–11) is H-Ser-Val-Ser-Glu-Ile-Gln-Leu-Met-His-Asn-Leu-NH_2. The following pseudo-undecapeptides were prepared: [Ala^1, 7,5-bTL^{3,4}, Nle^8, Arg^{11}]hPTH(1–11)NH_2 (**I**); [Ala^1, 7,5-bTL^{6,7}, Nle^8, Arg^{11}]hPTH(1–11)NH_2 (**II**); [Ala^1, Nle^8, 7,5-bTL^{9,10}, Arg^{11}]hPTH(1–11)NH_2 (**III**). In aqueous solution containing 20% TFE, only analogue **I** exhibited the typical CD pattern of the α-helical conformation. NMR experiments and molecular dynamics calculations located the α-helical stretch in the sequence Ile^5-His^9. The dipeptide mimetic unit 7,5-bTL induces a type III β-turn, occupying the positions $i-1$ and i of the turn. Analogue **II** exhibited an equilibrium between a type I β-turn and an α-helix, and analogue **III** did not show any ordered structure. Biological tests revealed poor activity for all analogues ($EC_{50} > 0.1$ mM). Apparently, the relative side-chain orientation of Val^2, Ile^5 and Met^8 can be critical for effective analogue-receptor interaction. Considering helicity as an essential property to obtain active PTH agonists, one must decorate the correctly positioned dipeptide mimetic azabicycloalkane scaffold with substitutions corresponding to the displaced amino acids. Copyright © 2007 European Peptide Society and John Wiley & Sons, Ltd.

Supplementary electronic material for this paper is available in Wiley InterScience at http://www.interscience.wiley.com/jpages/1075-2617/suppmat/

Keywords: PTH; NMR; peptide mimetics; molecular modeling

INTRODUCTION

Parathyroid hormone (PTH) is an 84-amino-acid peptide responsible for the regulation of calcium homeostasis in the body extracellular fluids. These activities are mediated through interaction with its cognate receptor, PTH1R, a G-protein-coupled seven transmembrane domain-containing receptor (GPCR) of class B. The *N*-terminal (1–34) fragment of PTH is fully active *in vivo*, and reproduces all biological responses characteristic of the native intact PTH [1]. Clinical studies have demonstrated that PTH(1–34) is a powerful bone anabolic agent capable of restoring bone mineral density. Recombinant human PTH(1–34) has been approved by FDA with the name of FORTEO (Teriparatide) to treat osteoporosis in postmenopausal women who are at high risk for fractures.

The prevailing view of the biologically relevant conformation of PTH(1–34) includes a flexible molecule with no tertiary structure. NMR analyses of PTH(1–34) analogues in a variety of polar and non-polar solvents suggest that the *N*-terminal portion of PTH, known to be responsible for receptor activation, contains a short α-helical segment from Ser^3 to Lys^{13}. This *N*-terminal helix is followed by a more stable *C*-terminal α-helical segment (from Arg^{20} to Val^{31}), in which the principal receptor binding domain is located. These two helices are separated by two hinge-like motifs located around positions 12 and 19 [2]. Previous studies demonstrated that enhancement of the α-helicity in the PTH(1–11) sequence (H-Ser-Val-Ser-Glu-Ile-Gln-Leu-Met-His-Asn-Leu-NH_2) yielded potent PTH(1–11)NH_2 analogues [3–5]. On the basis of mutagenesis studies

Abbreviations: Aib, α-amino butyric acid; Ac5c, amino-pentacyclo carboxylic acid; HBTU, 2-(1*H*-benzotriazole-1-yl)-1,1,3,3-tetramethyluronium hexafluorophosphate; HOBt, 1-hydroxybenzotriazole; DIPEA, diisopropylethyl amine; DMF, Dimethyl formamide; NMP, *N*-methyl pyrrolidone; HATU, 2-(1*H*-7-azabenzotriazole-1-yl)-1,1,3,3-tetramethyluronium hexafluorophosphate; HOAt, 1-hydroxy-7-azabenzotriazole; Ac_2O, acetic anhydride; TFA, trifluoroacetic acid; TIS, triisopropylsilane; EDT, ethanedithiol; PBS, phosphate buffered saline; BSA, bovine serum albumin.

*Correspondence to: E. Peggion, University of Padova, Department of Chemical Sciences, Institute of Biomolecular Chemistry, CNR, Italy; e-mail: evaristo.peggion@unipd.it

and on the position and shape of the binding sites for residues in position 2, 5 and 8, high helicity has been suggested to be essential for receptor activation [6,7]. Furthermore, location of residue 8 on the same face of the helix as Ile^5, as well as the position of Val^2 projecting towards the third extracellular loop (EC3), has been hypothesized to be fundamental requirements for the activation of PTH1R [6].

This work provides useful new information on the requirements for PTH ligand bioactivity and on general aspects of peptide mimetic design work. We synthesized and biologically and conformationally characterized three PTH-mimetic molecules, all containing 3*R*-carboxy-6*S*-amino-7,5-bicyclic thiazolidinlactam (7,5-bTL) (Figure 1), a polyol dipeptide mimetic derived from a carbohydrate precursor [8] which can mimic hydroxyl amino acids: [Ala^1, 7,5-$bTL^{3,4}$, Nle^8, Arg^{11}] hPTH(1–11) NH_2 (**I**); [Ala^1, 7,5-$bTL^{6,7}$, Nle^8, Arg^{11}] hPTH(1–11) NH_2 (**II**); [Ala^1, Nle^8, 7,5-$bTL^{9,10}$, Arg^{11}] hPTH(1–11) NH_2 (**III**). Introduction of conformational constraints into peptides can improve their activity and receptor binding selectivity [9–11]. This approach, applied to PTH(1–11) has already been shown to yield compounds with enhanced activity [12].

The dipeptide mimetic was inserted in strategic positions, in order to leave the side chain of the essential residues 2, 5 and 8 unmodified. The replacement of Met^8 with Nle^8 is known to be well tolerated, producing no loss of binding affinity [13,] and prevents methionine oxidation, which would result in a decrease in the biological response [14]. The replacement of Leu^{11} with Arg^{11} is known to enhance autoactivation [15] in the PTH1R/[Arg^{11}]PTH(1–11) tethered system, which lacks most of the extracellular *N*-terminal domain (N-ECD) of PTH1R, thus leading to the hypothesis that neither the 1–181 N-ECD of the receptor nor the *C*-terminal portion of PTH(1–34) is essential for bioactivity. Moreover, the presence of Arg^{11}/Har^{11} turned some analogues of PTH(1–11) into potential agonists [12,16], while analogues of PTH truncated at position 10 displayed poor binding and low activity [17].

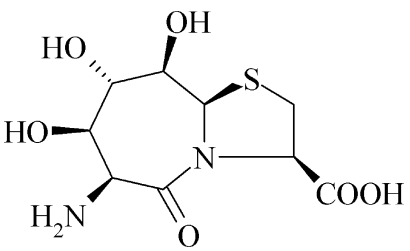

Figure 1 Structure of the rigidified dipeptide mimetic unit derived from 3*R*-carboxy-6*S*-amino-7,5-bicyclic thiazolidinlactam (7,5-bTL).

MATERIALS AND METHODS

Synthesis

The solid-phase synthesis of [Ala^1, 7, 5-$bTL^{3,4}$, Nle^8, Arg^{11}] hPTH(1–11)NH_2 (analogue **I**) is outlined in Scheme 1. The synthetic protocol for the other analogues is similar. The analogues were prepared using Fmoc methodology with Rink Amide MHBA resin (Novabiochem) (0.73 mmol/g loading) as a solid support [18]. The bicyclic lactam 7,5-bTL was prepared [8] and protected at the free amino group as fluorenyl carbamate. The first amino acid was anchored to the resin using the HBTU/HOBt/DIPEA protocol; the most common peptide coupling additive is HOBt, used either as a carbocation with another coupling agent or incorporated into a stand-alone reagent such as a uronium salt [19]. Such additions generally inhibit side reactions and reduce epimerization. In this case, we used HOBt as an auxiliary nucleophile. Deprotection of Fmoc from the α-amino groups was achieved under standard conditions, with 20% piperidine solution in DMF. The following amino acids were coupled in the same way. The coupling of 7,5-bTL was accomplished with the more potent condensation reagent HATU/HOAt/2,4,6-collidine [20–22]. For reasons yet unclear, 2,4,6-collidine as a base appears to be particularly suitable for systems derived from HOAt [20–22]. Because of the high synthetic value of 7,5-bTL, it was used in a stoichiometric amount with respect to the resin [23], and a longer reaction time was used to improve the yield of incorporation. After end-capping with Ac_2O, the next amino acid was introduced on the sterically hindered free amino group of the lactam using the same method and a large excess of reagents.

Peptide deprotection, cleavage from the resin and purification. The resin-bound peptide was treated with a deprotection and cleavage solution of TFA/EDT/TIS/water (94 : 2.5 : 1 : 2.5

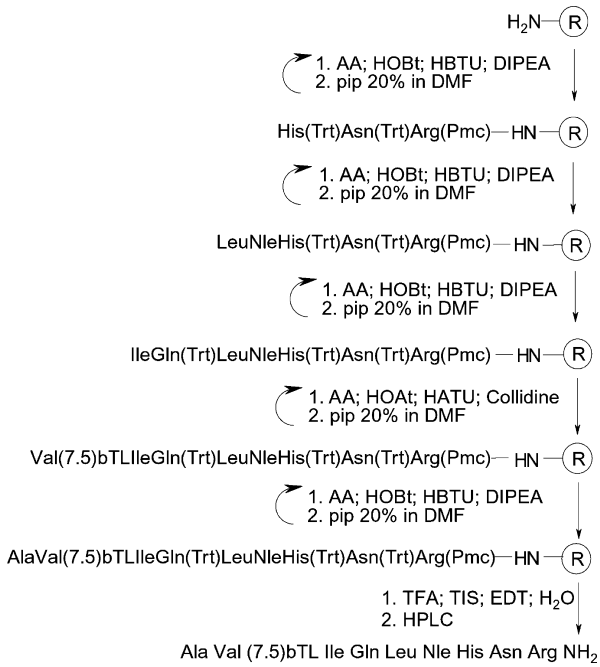

Scheme 1 Solid-phase synthesis of analogues **I**–**III** (analogue **I** is reported as an example of the synthetic protocol).

DOI: 10.1002/psc

v/v/v/v) at room temperature for 2 h. After filtration, the filtrate was concentrated under nitrogen and precipitated with methyl tert-butyl ether. Peptide purification was performed by reverse-phase HPLC on a Vydac C_{18} (218TP510) column. The peptide homogeneity (>95%) was determined by analytical HPLC using the same solvents with a linear gradient of 10–35% (v/v) acetonitrile over 25 min. Analogue **I**: Retention time (RT) = 13.27 min; yield after purification and lyophilization: 10%; Mass (ESI-MS) (M + H) m/z 1321.7. Analogue **II**: RT = 13.70 min; yield after purification and lyophilization: 11%; Mass (ESI-MS) (M + H) m/z 1298. Analogue **III:** RT = 13.61 min; yield after purification and lyophilization: 5%; Mass (ESI-MS) (M + H) m/z 1286.7.

Circular Dichroism

CD measurements were carried out on a JASCO J-715 spectropolarimeter interfaced with a PC. The CD spectra were acquired and processed using the J-700 program for Windows. All experiments were carried out at room temperature using HELLMA quartz cells with Suprasil windows and optical path lengths of 0.01 and 0.1 cm. All spectra were recorded using a bandwidth of 2 nm and a time constant of 8 s at a scan speed of 20 nm/min. The signal-to-noise ratio was improved by accumulating eight scans. Measurements were performed in the wavelength range 190–250 nm and the concentration of the peptides was in the range 0.07–1.07 mM. The peptides were analysed in aqueous solution containing 2,2,2-trifluoroethanol (TFE) 20% (v/v). The spectra are reported in terms of mean residue molar ellipticity (deg cm^2 $dmol^{-1}$). The helical content for each peptide was estimated according to the literature [24].

NMR Measurements and Molecular Modelling Calculations

NMR spectra were recorded at 298 K on a BRUKER AVANCE DMX-600 spectrometer. The experiments were carried out in H_2O/TFE-d_3 (4 : 1 v/v). The sample concentration was approximately 1 mM in 600 µl of solution. The water signal was suppressed by pre-saturation during the relaxation delay. The spin systems of all amino acid residues were identified using standard DQF-COSY [25] and CLEAN-TOCSY [26,27] spectra. In the latter case, the spin-lock pulse sequence was 70 ms long. The sequence-specific assignment was accomplished using the rotating-frame Overhauser enhancement spectroscopy (ROESY), using a mixing time of 150 ms. In all homonuclear experiments, the spectra were acquired by collecting 400–512 experiments, each one consisting of 32–256 scans and 4 K data points.

Spectral processing was carried out using XWINNMR. Spectra were calibrated against the TMS signal. Inter-proton distances were obtained by integration of the ROESY spectra using the AURELIA software package. The calibration was generally based on the geminal γ protons of Ile^5, set to a distance of 1.78 Å. This was not possible for analogue **II** because the cross-peak was partially overlapped with the diagonal. The calibration was then performed on the αH–βH distance of Ala^1, set to 2.73 Å. The offset correction was performed setting the B1-field value (2500 Hz) and the B1-frequency (*ca* 4.80 ppm), according to the formulas published by Bull [28].

Distance geometry (DG) and molecular dynamics (MD) calculations were carried out using the simulated annealing (SA) protocol of the X-PLOR 3.0 program. For distances involving equivalent or non-stereo-assigned protons, r^{-6} averaging was used. The MD calculations involved a minimization stage of 100 cycles, followed by SA and a refinement stage. The SA consisted of 30 ps of dynamics at 1500 K (10 000 cycles, in 3 fs steps) and of 30 ps of cooling from 1500 to 100 K in 50 K decrements (15 000 cycles, in 2 fs steps). The SA procedure, in which the weights of ROE and non-bonded terms were gradually increased, was followed by 200 cycles of energy minimization. In the SA refinement stage, the system was cooled from 1000 to 100 K in 50 K decrements (20 000 cycles, in 1 fs steps). Finally, the calculations were completed with 200 cycles of energy minimization using an ROE force constant of 50 cal/(mole Å). One hundred and fifty structures were generated for each analogue, and the 20 minimum energy structures containing no distance constraint violation (<0.5 Å from the integration value) were chosen for conformational study, using the INSIGHT II and MOLMOL (version 2.6) programs with a SILICON GRAPHICS O2 R 10 000 workstation. The secondary structure was determined using H-bond analysis, dihedral angle calculations and the Kabsch and Sander algorithm [29].

Activity Assays

C20 HEK293 cells stably expressing the PTH1R were seeded at 10^5 cells/well in collagen-coated 24-well plates. Twenty-four hours later, the cells were treated with FuGENE 6 Transfection Reagent (1 µl/well) and CRE-luc plasmid (0.2 µg/well) in 0.5 ml/well serum-free Opti-Mem 1, according to the manufacturer's procedure.

Eighteen hours after transfection, the medium was replaced with 225 µl/well of Dulbecco's Modified Eagle Medium. To this, 25 µl/well of a solution of peptide in PBS/0.1% BSA was added, and the cells were incubated for 4 h at 37 °C, yielding maximal response to luciferase. Each peptide concentration was used in triplicate. The medium was aspirated and the cells were washed once with PBS pH 7.4 (250 µl/well). The cells were lysed by addition of 200 µl of Passive Lysis Buffer per well and gentle shaking for 5 min. The suspension was then transferred to labelled low-binding eppendorf tubes and centrifuged for 2 min, and 80 µl of the supernatant was transferred into labelled glass tubes.

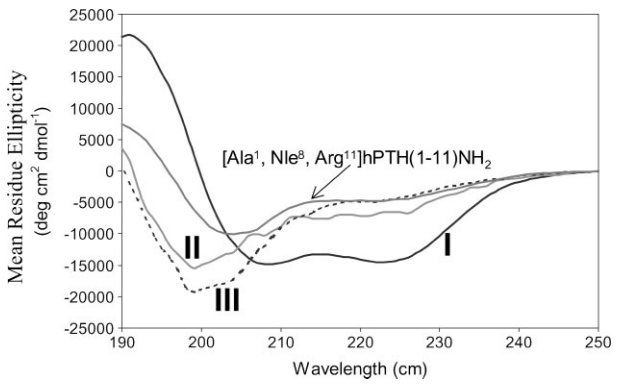

Figure 2 CD spectra in aqueous solution containing 20% TFE(v/v). Concentrations: 1.074 mM (**I**); 0.428 mM (**II**); 0.066 mM (**III**). [Ala^1, Nle^8, Arg^{11}]hPTH(1–11)NH_2 is included as a reference (1.240 mM).

DOI: 10.1002/psc

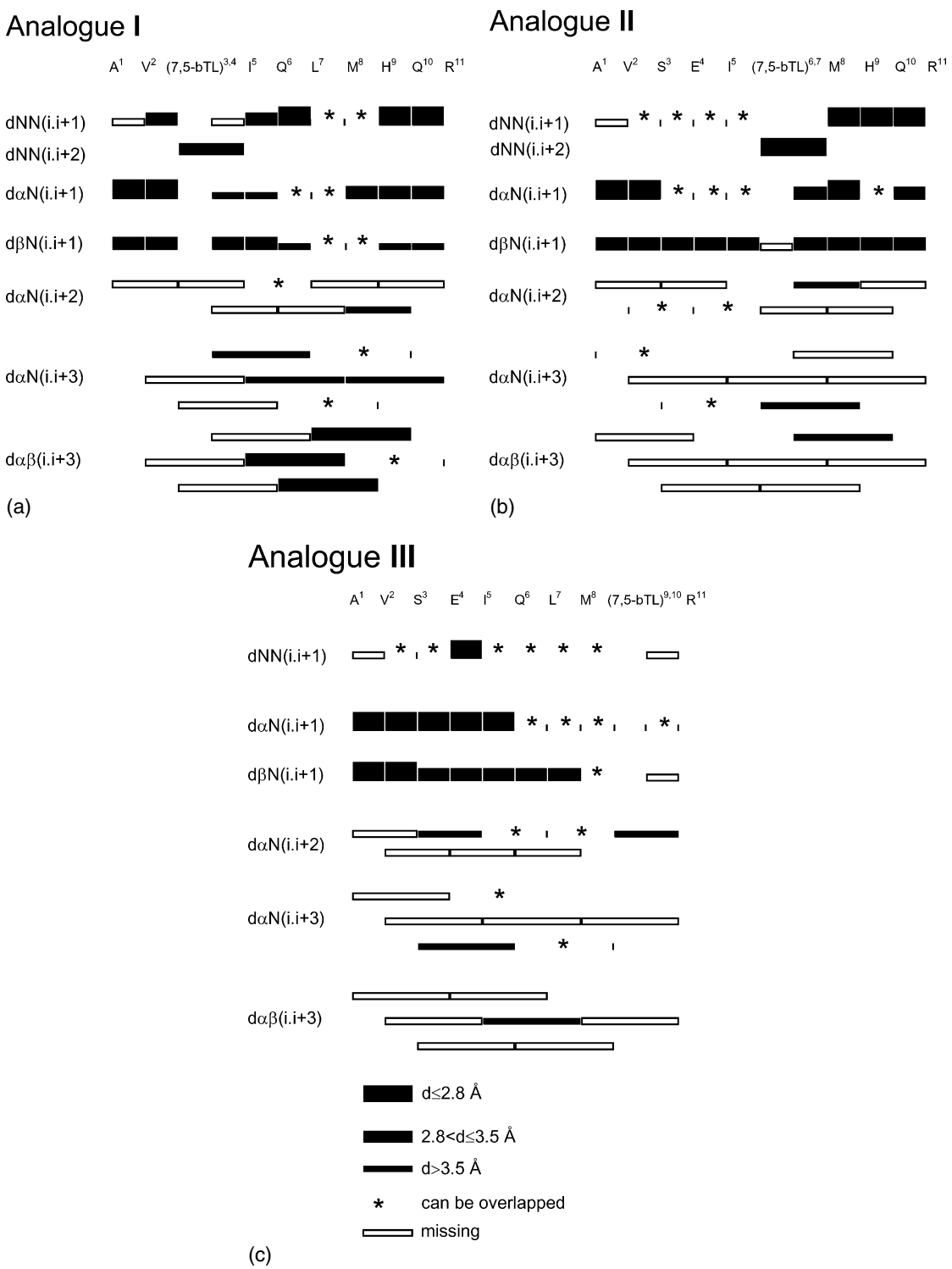

Figure 3 Summary of ROESY connectivities of analogues **I**–**III**. Peaks are grouped into three classes, based upon their integrated volumes.

Luciferase activity was measured on a Lumat LB 9507 luminometer (EG&G Berthold). This instrument automatically injects pre-defined volumes of two solutions, A and B, with the compositions described below. Initially, a Solution 0 was prepared, containing glycylglycine 25 mM, $MgSO_4$ 15 mM and ethyleneglycol-bis(β-aminoethyl ether)-*N*, *N*, *N*′, *N*′-tetraacetic acid (EGTA) 4 mM in deionized water. Solution A was 0.2 mM D-luciferin in Solution 0. Solution B was K_3PO_4 0.02 M, ATP 2.5 mM and dithiothreitol 1 mM in Solution 0. The instrument was calibrated to add 100 µl of Solution A and 300 µl of Solution B to a sample tube, and the measurement was performed for 20 s. The mean read out from three wells with identical peptide concentrations was used to present the data.

DOI: 10.1002/psc

RESULTS AND DISCUSSION

CD Results

The conformational properties of the three peptide mimetics were initially investigated by CD in TFE/water 20%, as in our previous experiments on potentially bioactive PTH-derived peptides [5]. The spectra in the far-UV region were collected at room temperature and are shown in Figure 2. The spectrum of analogue **I** exhibits the typical shape usually associated with the α-helical conformation, showing two negative bands of comparable magnitude near 222 and 208 nm and a stronger positive band near 190 nm. For analogue **I,** the α-helix content is estimated at 66% [24]. The presence of β-turns is not excluded, since their CD patterns qualitatively resembles that of an α-helix [30]. Analogues **II** and **III** are characterized by negative bands at ~200 nm, showing a lower content of ordered structure with respect to analogue **I**. However, the shape of these curves does not exclude the presence of some contribution of α-helix or β-turn for these analogues, as well as the co-presence of two or more conformations. No concentration dependence of the CD profiles was observed for any of these analogues (data not shown).

Resonance Assignment and NMR Solution Structures

Complete proton resonance assignment was possible using the standard procedure [31]. Tables S1–S3 in the Supporting Information contain the full chemical shift information. Figure 3 summarizes the sequential and medium range ROE connectivities observed for analogues **I**–**III** in 20% v/v TFE-d_3. For analogue **I**, the observation of continuous $d_{NN}(i, i+1)$ contacts together with characteristic $d_{\alpha N}(i, i+3)$ and $d_{\alpha\beta}(i, i+3)$ ROEs indicates the presence of an α-helix spanning the sequence Ile^5-Arg^{11}. Analogue **II** contains a smaller number of these ROE interactions, and only in the *C*-terminal portion, starting from Nle^8. Analogue **III** shows only one $d_{NN}(i, i+1)$ interaction because of a large number of overlapped peaks. The small number of $d_{\alpha N}(i, i+3)$ and $d_{\alpha\beta}(i, i+3)$ connectivities indicates the absence of significant secondary structure.

Figure 4 shows the chemical shift differences of the αH protons with respect to the values of the random coil conformation [32] and identifies a short helical segment in the sequence Ile^5-Nle^8 for analogue **I** (negative values $\geq$0.1 ppm), while analogues **II** and **III** exhibit no helical structure. The inactive reference peptide [Ala^1, Nle^8, Arg^{11}]hPTH(1–11)NH$_2$ has a reduced preference for the α-helical conformation with respect to analogue **I**, as found in the CD spectra (Figure 2), indicating that the insertion of 7,5-bTL stabilizes the secondary structure, at least under the conditions used here.

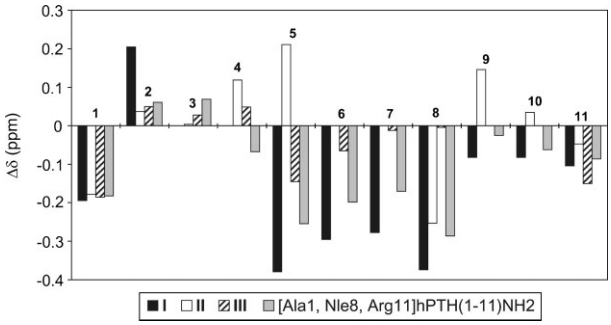

Figure 4 Chemical shift differences of the αH protons of analogues **I**–**III**. The data relative to [Ala^1, Nle^8, Arg^{11}]hPTH(1–11)NH$_2$ are also included as a reference.

Table 1 Structural statistics for analogues **I**–**III**

	Analogue **I**	Analogue **II**	Analogue **III**
Experimental NMR constraints			
Intra-residue ($i-j=0$)	45	46	34
Sequential ($\|i-j\|=1$)	32	20	22
Medium range ($2 \leq \|i-j\| \leq 4$)	16	11	3
Total	95	77	59
⟨RMSD⟩ from experimental constraints (Å)			
Distance	0.088 ± 0.010	0.116 ± 0.002	0.116 ± 0.004
Atomic ⟨RMSD⟩ (Å)			
Backbone (1–11)	0.7 ± 0.3	2.0 ± 1.1	2.2 ± 1.0
Heavy atoms (1–11)	1.4 ± 0.4	3.2 ± 1.2	3.3 ± 1.1
Mean energy (kcal/mol)			
E_{tot}	72 ± 10	95 ± 3	83 ± 3
E_{bonds}	3.3 ± 0.4	6.0 ± 0.3	4.3 ± 0.4
E_{angles}	25.5 ± 1.1	27.9 ± 1.3	28 ± 2
E_{NOE}	37 ± 8	51.3 ± 1.7	43 ± 3

DOI: 10.1002/psc

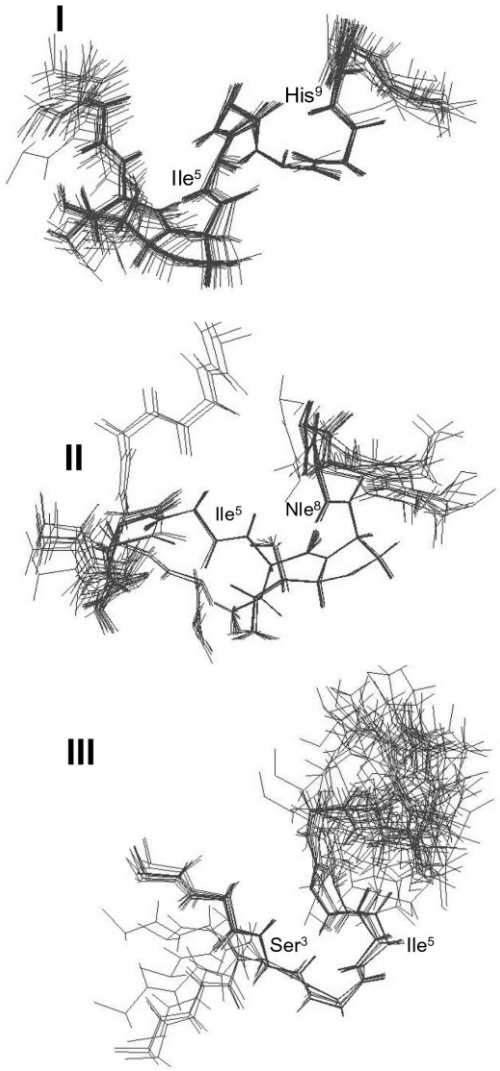

Figure 5 Superimposition of the ensembles of calculated structures of analogues **I**–**III**. Heavy backbone atoms of the sequences indicated were superimposed.

Structure Calculations

The experimental NMR constraints used in the structure calculations are reported in Table 1. The root mean-square deviation (RMSD) values from experimental constraints and the atomic RMSD[33] among the various structures are lower for analogue **I**, thus confirming a better defined secondary structure with respect to analogues **II** and **III**.

The mean values of the φ and ψ dihedral angle for all residues of analogue **I** were distributed in energetically acceptable regions, with angular order parameter (OP) values >0.95 [33], except for Ala[1], Val[2] and Arg[11] (see Figures S1–S3 in the Supporting Information). OPs for analogues **II** and **III** show that the dihedral angles φ and ψ are not very well defined for residues preceding the peptide mimetic moiety, indicating that the dipeptide-mimetic unit 7,5-bTL disrupts the tendency to form an ordered structure in the immediately preceding sequence. In fact, analogue **III** appears to be completely random (see Figure S3 in the Supporting Information). The superimposition of the ensemble of the low-energy structures of the three peptides is shown in Figure 5. A schematic representation of one of the lowest energy structures of analogues I–III is presented in Figure S4 in the Supporting Information.

It has been shown that 7,5-bTL can occupy the i to $i+1$ positions of type I and type II β-turns in cyclic hexapeptides [34]. In analogue **I**, we found a type III β-turn involving residues 4–7 (Table 2), immediately following the 7,5-bTL[3,4] residue. The β-turn can therefore be favoured by the dipeptide mimetic unit. The location of the β-turn is further supported by the H-bond analysis, which indicated that a (CO^4–NH^7) H-bond involving the backbone atoms occurs in 11 out of 20 structures (Table 3). Furthermore, there are significant occurrences of (i, $i+4$) H-bonds with $i=4$,

Table 2 Average values of torsion angles ϕ and ψ and relative standard deviations resulting from the 20 lowest energy structures calculated for analogues **I**–**III**

	Analogue I			Analogue II			Analogue III		
	Residue	ϕ_m (°)	ψ_m (°)	Residue	ϕ_m (°)	ψ_m (°)	Residue	ϕ_m (°)	ψ_m (°)
1	Ala	—	140 ± 30	Ala	—	149 ± 4	Ala	—	161 ± 9
2	Val	−70 ± 90	85 ± 6	Val	−111 ± 8	−30 ± 4	Val	−117 ± 2	164.3 ± 1.1
3	7,5-bTL	−154 ± 3	−100.8 ± 0.3	Ser	0 ± 40	−70 ± 40	Ser	−100 ± 40	173 ± 16
4	7,5-bTL	−77.9 ± 0.5	−42.3 ± 1.1	Glu	−80 ± 20	−40 ± 100	Glu	−70 ± 30	−37 ± 3
5	Ile	−47 ± 2	−39 ± 4	Ile	−90 ± 20	172 ± 3	Ile	−129 ± 10	−16 ± 4
6	Gln	−85 ± 6	−19 ± 12	7,5-bTL	155 ± 8	−105.0 ± 0.4	Gln	−50 ± 30	170 ± 70
7	Leu	−83 ± 13	−10 ± 8	7,5-bTL	−78.1 ± 0.4	−45.0 ± 0.9	Leu	40 ± 70	−68 ± 18
8	Nle	−109 ± 12	−27 ± 12	Nle	−41.4 ± 1.4	−25.3 ± 1.8	Nle	−50 ± 50	75 ± 10
9	His	−93 ± 12	−13 ± 6	His	−137 ± 8	−40 ± 40	7,5-bTL	−159.7 ± 0.9	−100.7 ± 0.9
10	Asn	−107 ± 10	0 ± 9	Asn	−80 ± 50	−30 ± 14	7,5-bTL	−76.7 ± 0.5	2.3 ± 0.9
11	Arg	−120 ± 40	0 ± 120	Arg	−10 ± 70	—	Arg	50 ± 110	—

DOI: 10.1002/psc

5 and 6. This means that in analogue **I** 7,5-bTL is able to induce a 3_{10} helix loop which develops into an α-helical structure. This hypothesis agrees with the calculation of a secondary structure with the Kabsch and Sander algorithm [29], which indicates for analogue **I** an α-helical segment in the region Ile^5–His^9. The same calculations for analogues **II** and **III** show no preference for secondary structure.

(i, $i+4$) H-bonds with $i = 6$, 7 are present with a 50% frequency in analogue **II** (Table 3), and suggest a certain degree of structural order in the 7,5-$bTL^{6,7}$-Asn^{10} region, despite the CD analysis which indicates a non-helical preference. This apparent discrepancy can be explained by the presence of a (CO^7–NH^{10}) H-bond in 5 out of 20 structures, which leads to the hypothesis of a β-turn. The mean values for dihedral angles φ and ψ at position 8 and 9 (Table 2) are reasonable for a type I β-turn, and are even better if calculated only for the five (CO^7–NH^{10}) H-bond-containing structures: φ^8, ψ^8 and φ^9 have a smaller relative error and the value for ψ^9 is better ($\psi^9 = +26 \pm 2^\circ$).

Comparing these data with the secondary chemical shift values and the CD analysis, we found that analogue **II** presents an equilibrium between α-helical conformation and β-turn structure. There are no H-bonds involving the backbone atoms in analogue **III** and the same behaviour can be seen also in analogues **I** and **II** for residues preceding 7,5-bTL. Our hypothesis is that 7,5-bTL, because of its sterically hindered structure, prevents the formation of an ordered conformation in the segment preceding its position. Therefore, its closer proximity to the amino terminus in analogue **I** relative to analogues **II** and **III** allows the presence of a stable helical conformation in the first but not in the last two analogues.

The bioactivity assays on C20 HEK293 cells (Table 4) indicate that analogues **I**–**III** are poorly active in comparison with the fully active PTH(1–34). Considering that [Ala^1, Nle^8, Arg^{11}]hPTH(1–11)NH_2 is also inactive, the 7,5-bTL substitution does not necessarily imply a reduction in activity.

However, there are substitutions in PTH(1–11) analogues that generate potent agonists of PTH(1–34), with EC_{50} values in the nanomolar range [4,5]. Apparently,

Table 3 Backbone H-bond analysis carried out on the 20 minimum energy structures of each analogue, fixing 2.4 Å as the maximum distance between the donor (H) and the acceptor (O) and 45° as the maximum deviation from the planar angle (180°) between N–H and C=O

	Analogue I	
i	H-bond (i, $i+3$) occurrence (%)	H-bond (i, $i+4$) occurrence (%)
Analogue I		
4	55	25
5	0	25
6	0	35
8	5	0
Analogue II		
2	45	0
6	0	45
7	25	50
Analogue III		
5	10	0
6	5	0

Table 4 Biological activity of PTH(1–11) analogues **I**–**III** (cAMP stimulation responses in C20 cells, Luciferase reporter assays). Data relating to [Ala^1, Nle^8, Arg^{11}]hPTH(1–11)NH_2 and PTH(1–34)NH_2 are included as reference

Analogue	EC_{50} (nM)
[Ala^1, 7,5-$bTL^{3,4}$, Nle^8, Arg^{11}]h PTH(1–11)NH_2	$>10^5$
[Ala^1, 7,5-$bTL^{6,7}$, Nle^8, Arg^{11}]hPTH(1–11)NH_2	$>10^5$
[Ala^1, Nle^8, 7,5-$bTL^{9,10}$, Arg^{11}]hPTH(1–11)NH_2	$>10^5$
[Ala^1, Nle^8, Arg^{11}]hPTH(1–11)NH_2	$>10^5$
PTH(1–34)NH_2	1.03 ± 0.12

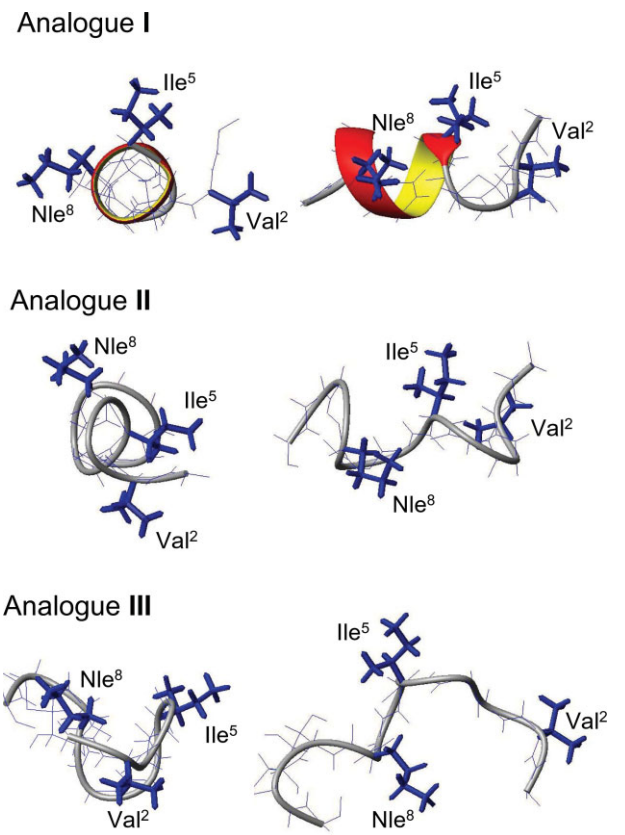

Figure 6 Comparison of top (left) and side (right) views of the relative orientation of Val^2, Ile^5 and Nle^8 side chains in representative structures of analogues **I**–**III**.

DOI: 10.1002/psc

our efforts to minimize the PTH pharmacophore by introducing conformational constraint into the backbone of PTH(1–11) as a general strategy to optimize the bioactive conformation leaving unmodified the clearly critical residues, i.e. Val^2, Ile^5 and Met^8/Nle^8, were not sufficient to generate potent PTH-like analogues. In fact, analogue **I** is not active although 7,5-bTL in position (3,4) can putatively mimic the Ser^3 and to some extent the Glu^4 side chains, and permits the presence of helical structural elements from position 4 on. These results underline that stabilization of a helical segment at the *N*-terminus of PTH(1–11) analogues, as observed in analogue **I**, may be necessary but not sufficient to generate a bioactive PTH-like compound. It is possible that the side chain of Glu^4 is not well mimicked by 7,5-bTL, or that substitution with the peptide mimetic between the residues Val^2 and Ile^5 constrains the side chains in an unfavourable interaction with the receptor. To investigate the relative side-chain orientation of the critical residues 2, 5 and 8, we used the ligand-tethered PTH1R model [6]. Previous studies had suggested that PTH1R could adopt at least several different conformations, and that neither the (12–34) portion of PTH(1–34) nor the *N*-terminal extracellular domain of the receptor was required for high ligand–receptor affinity. Analogues such as [$Ac5c^1$, Aib^3, Gln^{10}, Arg^{11}]PTH(1–11)NH_2 are in a well-defined α-helical structure and show high activity in the luciferase reporter assay on HEK 293 cells [5], and PTH1R lacking the *N*-terminus is constitutively active if PTH(1–11) is tethered to it through a four glycine linker [15]. We hypothesized that analogues **I**–**III** interact with PTH1R through the same conformation assumed by the receptor in the tethered model.

An effective ligand-PTH1R interaction occurs if the so-called bioactive conformation can display the side chains in the correct topology. Figure 6 pictorially explains the different side-chain orientations of the three analogues with respect to the conformation and side-chain topology of PTH(1–11) in the ligand-tethered PTH1R model. In the latter case, the side chain of Nle^8 (replacing Met^8) is on the same face of the *N*-terminal helix as Ile^5 and therefore can share the same deep hydrophobic pocket in PTH1R [6]. For analogue **III**, in which no secondary structure was detected, the PTH-like bioactive topology cannot be achieved. In analogue **II**, the type I β-turn – α-helix conformation equilibrium probably does not favour the interaction with the receptor. Analogue **I** presents a spatial orientation of the Val^2, Ile^5 and Nle^8 side chains significantly different with respect to PTH(1–11). Taken together, these results suggest that a very stable helix encompassing these residues appears to be fundamental, although not sufficient, for PTH-like ligand-PTH1R interaction.

In conclusion, in this work we introduced a dipeptide mimetic unit to generate PTH analogues based on the *N*-terminal miniaturized sequence, which was previously demonstrated to effectively activate the PTH1R. The procedure to insert a dipeptide mimetic unit into the PTH-derived sequence is fully described. In particular, we demonstrated that 7,5-bTL can occupy the $i-1$ and i positions of a type III β-turn, inducing a 3_{10} helix loop which can develop into a α-helix. Considering helicity as fundamental for PTH active agonists, further use of these sugar-based mimetics can be strategic, because the azabicycloalkane backbone can be functionalyzed to mimic specific side chains, preserving the helical secondary structure and reproducing the topology essential for productive ligand-PTH1R interaction.

Supplementary Material

Supplementary electronic material for this paper is available in Wiley InterScience at: http://www.interscience.wiley.com/jpages/1075-2617/suppmat/

For analogues **I** – **III**: proton resonance frequency tables; angular order parameter graphics; schematic representation of one of the lowest energy structures.

Acknowledgements

The authors thank MIUR, Ministry of Education and University of Italy, CNR, the National Research Council of Italy and Abiogen S.p.A. for financial support and Dr. Barbara Biondi for assistance in mass spectroscopy.

REFERENCES

1. Chorev M, Rosenblatt M. *The Parathyroids*. Raven Press: New York, 1994; 139–156.
2. Scian M, Marin M, Bellanda M, Tou L, Alexander JM, Rosenblatt M, Chorev M, Peggion E, Mammi S. Backbone dynamics of human parathyroid hormone (1-34): flexibility of the central region under different environmental conditions. *Biopolymers* 2006; **84**: 147–160.
3. Shimizu M, Petroni BD, Khatri A, Gardella TJ. Functional evidence for an intramolecular side chain interaction between residues 6 and 10 of receptor-bound parathyroid hormone analogues. *Biochemistry* 2003; **42**: 2282–2290.
4. Tsomaia N, Pellegrini M, Hyde K, Gardella TJ, Mierke DF. Toward parathyroid hormone minimization: conformational studies of cyclic PTH(1-14) analogues. *Biochemistry* 2004; **43**: 690–699.
5. Barazza A, Wittelsberger A, Fiori N, Schievano E, Mammi S, Toniolo C, Alexander JM, Rosenblatt M, Peggion E, Chorev M. Bioactive N-terminal undecapeptides derived from parathyroid hormone: the role of alpha-helicity. *J. Pept. Res.* 2005; **65**: 23–35.
6. Monticelli L, Mammi S, Mierke DF. Molecular characterization of a ligand-tethered parathyroid hormone receptor. *Biophys. Chem.* 2002; **95**: 165–172.
7. Shimizu M, Potts JT Jr., Gardella TJ. Toward parathyroid hormone minimization: conformational studies of cyclic PTH(1-14) analogues. *J. Biol. Chem.* 2000; **275**: 21836–21843.
8. Geyer A, Moser E. Polyol peptidomimetics. *Eur. J. Org. Chem.* 2000; **7**: 1113–1120.
9. Hirschmann R. Medicinal chemistry in the golden age of biology: lessons from steroid and peptide research. *Angew. Chem. Int. Ed.* 1991; **30**: 1278–1301.
10. Gante J. Peptidomimetics – tailored enzyme inhibitors. *Angew. Chem. Int. Ed.* 1994; **33**: 1699–1720.

11. Kessler H, Diefenbach B, Finsinger D, Geyer A, Gurrath M, Goodman SL, Hölzemann G, Haubner R, Jonczyk A, Muller G, Graf v. Roedern E, Wermuth J. Design of superactive and selective integrin receptor antagonists containing the RGD sequence. *Lett. Pept. Sci.* 1995; **2**: 155–160.
12. Shimizu M, Guo J, Gardella TJ. Parathyroid hormone (PTH)-(1-14) and -(1-11) analogs conformationally constrained by alpha-aminoisobutyric acid mediate full agonist responses via the juxtamembrane region of the PTH-1 receptor. *J. Biol. Chem.* 2001; **276**: 49003–49012.
13. Rosenblatt M, Goltzmann D, Keutmann HT, Tregear GW, Potts JT Jr. Chemical and biological properties of synthetic, sulfur-free analogues of parathyroid hormone. *J. Biol. Chem.* 1976; **251**: 159–164.
14. Frelinger AL, Zull JE. Oxidized forms of parathyroid hormone with biological activity. Separation and characterization of hormone forms oxidized at methionine 8 and methionine 18. *J. Biol. Chem.* 1984; **259**: 5507–5513.
15. Shimizu M, Carter PH, Gardella TJ. Autoactivation of type-1 parathyroid hormone receptors containing a tethered ligand. *J. Biol. Chem.* 2000; **275**: 19456–19460.
16. Shimizu M, Carter PH, Khatri A, Potts JT Jr., Gardella TJ. Enhanced activity in parathyroid hormone-(1-14) and -(1-11): novel peptides for probing ligand-receptor interactions. *Endocrinology* 2001; **142**: 3068–3074.
17. Shimizu M, Dean T, Khatri A, Gardella TJ. Amino-terminal parathyroid hormone fragment analogs containing alpha,alpha-di-alkyl amino acids at positions 1 and 3. *J. Bone Miner. Res.* 2004; **19**: 2078–2086.
18. Carpino LA, El-Faham A, Minor CA, Albericio F. Advantageous applications of azabenzotriazole (triazolopyridine)-based coupling reagents to solid-phase peptide synthesis. *J. Chem. Soc., Chem. Commun.* 1994; 201–203.
19. Knorr R, Trzeciak A, Bannwarth W, Gillessen D. New coupling reagents in peptide chemistry. *Tetrahedron Lett.* 1989; **30**: 1927–1930.
20. Carpino LA. 1-Hydroxy-7-azabenzotriazole. An efficient peptide coupling additive. *J. Am. Chem. Soc.* 1993; **115**: 4397–4398.
21. Carpino LA, El-Faham A, Albericio F. Efficiency in peptide coupling: 1-hydroxy-7-azabenzotriazole vs 3,4-dihydro-3-hydroxy-4-oxo-1,2,3-benzotriazine. *J. Org. Chem.* 1995; **60**: 3561–3564.
22. Carpino LA, El-Faham A. Effect of tertiary bases on O-benzotriazolylluronium salt-induced peptide segment coupling. *J. Org. Chem.* 1994; **59**: 695–698.
23. Belvisi L, Bernardi A, Checchia A, Manzoni L, Potenza D, Scolastico C, Castorina M, Cupelli A, Giannini G, Carminati P, Pisano C. Potent integrin antagonists from a small library of RGD-including cyclic pseudopeptides. *Org. Lett.* 2001; **3**: 1001–1004.
24. Yang JT, Wu CS, Martinez HM. Calculation of protein conformation from circular dichroism. *Meth. Enzymol.* 1986; **130**: 208–269.
25. Rance M, Sørensen OW, Bodenhausen G, Wagner G, Ernst RR, Wüthrich K. Improved spectral resolution in COSY ^{1}H NMR spectra of proteins via double quantum filtering. *Biochem. Biophys. Res. Commun.* 1983; **117**: 479–485.
26. Bax A, Davis DG. MLEV-17-based two-dimensional homonuclear magnetization transfer spectroscopy. *J. Magn. Reson.* 1985; **65**: 355–360.
27. Griesinger C, Otting G, Wüthrich K, Ernst RR. Clean TOCSY for proton spin system identification in macromolecules. *J. Am. Chem. Soc.* 1988; **110**: 7870–7872.
28. Bull TE. ROESY relaxation theory. *J. Magn. Reson.* 1988; **80**: 470–481.
29. Kabsch W, Sander C. Dictionary of protein secondary structure: pattern recognition of hydrogen-bonded and geometrical features. *Biopolymers* 1983; **22**: 2577–2637.
30. Rose GD, Gierasch LM, Smith JA. Turns in peptides and proteins. *Adv. Protein Chem.* 1985; **37**: 1–109.
31. Wüthrich K. *NMR of Proteins and Nucleic Acids*. John Wiley & Sons: New York, 1986; 117–175.
32. Pastore A, Saudek V. The relationship between chemical shift and secondary structure in proteins. *J. Magn. Reson.* 1990; **90**: 165–176.
33. Hyberts SG, Goldberg MS, Havel TF, Wagner G. The solution structure of eglin c based on measurements of many NOEs and coupling constants and its comparison with X-ray structures. *Protein Sci.* 1992; **1**: 736–751.
34. Tremmel P, Geyer A. Coupled hydrogen-bonding networks in polyhydroxylated peptides. *Angew. Chem. Int. Ed.* 2004; **43**: 5789–5791.

DOI: 10.1002/psc